Spoof Plasmon Polaritons for NDE Applications an Experimental Demonstration

William C. Wilson
Nondestructive Evaluation Sciences Branch
NASA Langley Research Center
Hampton, VA, USA
William.C.Wilson@nasa.gov

Katelyn R. Brinker
Electrical and Computer Engineering Dept.
Iowa State University
Ames, IA, USA
brinker@iastate.edu

***Abstract*— NASA is exploring the use of microwave spoof plasmon polaritons to detect defects in metallic structures. This work investigates the detection of simulated defects in the form of aluminum wires as small as 1.6 mm diameter and 2 mm long that are placed in a grooved aluminum test article. The inclusions simulate manufacturing defects, and the sum of the delta impedance is shown to increase with increasing volume of added metal. Based on the results, a threshold value of 50Ω has been proposed for defect detection. In addition to detecting defects, the technique also estimates the volume of the defect.**

Keywords—— Microwave, Spoof Plasmon Polaritons, Electromagnetic; Surface Waves, NDE.

I. Introduction

NASA's Advanced Air Transport Technology (AATT) project is investing in revolutionary improvements in economic and environmental performance of subsonic fixed wing transport aircraft. In addition to investigating ultra-efficient wings, novel propulsion-airframe integration, and hybrid propulsion, AATT is also exploring the use of metal flow forming technology that offers significant reduction in cost, weight, and manufacturing time by reducing part count and eliminating lap joints and rivets (fasteners) that create structural defects and load discontinuities [1]. In November of 2018 NASA held a workshop on "Materials and Methods for Rapid Manufacturing for Commercial and Urban Aviation" [2]. Flow forming of metal was one of the explored technologies. Another important area addressed was the need for developing improved capabilities for nondestructive evaluation (NDE) and in-situ monitoring. One challenge associated with scaling up the flow forming process is the formation of defects during the forming process [3]. Accordingly, defect detection and location could prove critical in reducing component inspection times. To achieve this goal, electromagnetic surface waves called spoof plasmon polaritons are being investigated for NDE of metallic corrugated structures.

Spoof plasmon polaritons are electromagnetic surface waves that exhibit a non-radiative mode where the energy of the mode is concentrated at the interface, and it decays exponentially from the interface between a dielectric and a metal [4]. The spoof plasmon polaritons act as a series chain of microwave cavity resonators. As stated by Brock, "Any array of cavities with subwavelength geometry that individually support a resonance, such as a waveguide mode, can be used as a metamaterial structure that will support a surface wave." [4] Microwave resonators can be described using basic electrical properties such as the electrical impedance. For this effort, the characteristic impedance is calculated from the S-parameters which are measured using a network analyzer. Anything that is placed within the grooves of the plasmon grating will affect the impedance due either to the change of the cavity shape and/or a change of the dielectric coefficient. Therefore, our hypothesis is that any material added to the ideal grating will cause changes in the impedance, and that these changes can be used to indicate defects in manufacturing if the changes are caused by the addition of unintentional metal during manufacturing. Future work will investigate voids or missing material.

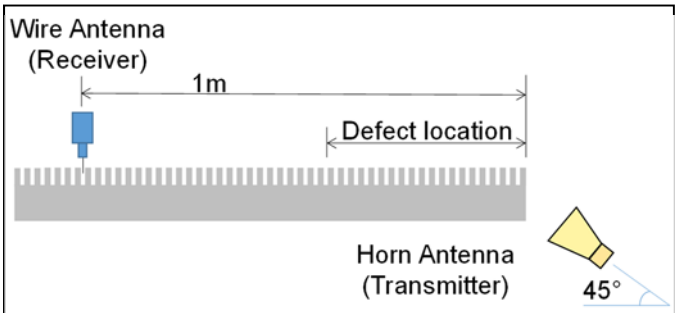

Fig. 1. Test setup for spoof plasmon polaritons showing the horn antenna, wire coaxial antenna, and grooved test specimen.

Spoof plasmon polaritons have been demonstrated in various corrugated or grooved structures such as rack gears. Also, these modes have been shown in non-rectangular teeth structures such as tapered grooves [5], rounded and V shaped grooves [6], triangular teeth [7] and trapezoidal shaped gear teeth [8]. Plasmons can travel in curves and in circles such as in ring resonator plasmons [8, 9]. Application of the technique to rounded corrugations were demonstrated in [10]. Fan shaped resonators have also been developed [11]. Even slotted structures and discs on a central cylinder can support plasmons [12].

Recently, spoof plasmon polaritons have been used for non-destructive testing (NDT). For instance, spoof plasmon polaritons have been used to detect defects in 3D printed waveguides [13].

This work is funded by NASA Advanced Air Transport Technology (AATT), which is part of the Advanced Air Vehicles Program (AAVP) under NASA's Aeronautics Research Mission Directorate (ARMD).

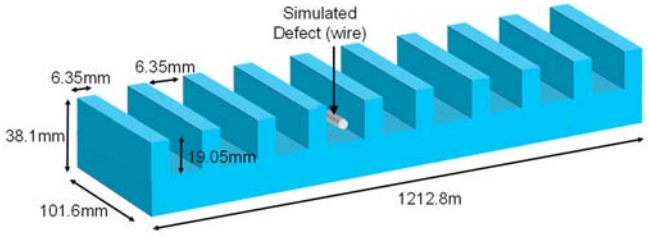

Fig. 2. Test specimen, aluminum (T6061), with a wire as a simulate defect.

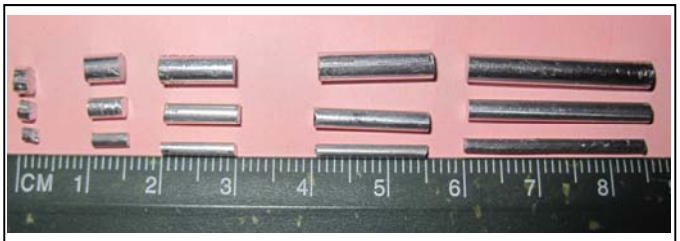

Fig. 4. defects: solid aluminum wires that are 2, 5, 10, 15, and 25 mm long and are 1.6, 2.3 and 3.1 mm diameter.

In addition, a method of using spoof plasmons to detect voids in dielectric materials has been demonstrated [14]. A flexible spoof plasmonic device that can detect defects in metal and non-metallic composites has been developed [15]. Another flexible Spoof plasmonic device uses a water filled tube to detect defects in non-metallic composites like PVC pipes [16].

In this paper we test the previously mentioned hypothesis (that any material added to the ideal grating will cause changes in the impedance, and that these changes can be used to indicate defects in manufacturing if the changes are caused by the addition of unintentional metal during manufacturing) by demonstrating that the electrical impedance of the spoof plasmon polariton can be used to detect defects.

II. Experimental Setup

The spoof plasmon polaritons system consists of a horn antenna (A H Systems SAS-571 double ridged horn antenna 700 MHz to 18 GHz) which is connected to a Keysight FieldFox N9918A 30 KHz to 26.5 GHz vector network analyzer, and a 31 mm long coaxial wire antenna (Fig. 1). The test specimen is a grooved aluminum (T6061) block that is 1212.8 mm long 101.6 mm wide and 38.4 mm high (Fig. 2). The grooves are 19.05 mm deep, 6.35 mm wide, and are spaced every 6.35 mm. The coaxial antenna is aligned vertically and is located in the middle of the groove located 1m from the horn antenna, and 0.7 mm from the bottom of the groove. The horn antenna is located 31 mm below end of the test specimen, at a 45° angle.

The network analyzer raw data is 10001 points of all four of the scatter (S) parameters (S_{11} S_{21} S_{12} S_{22}) versus frequency from 2.9 GHz to 3.3 GHz. Each complex S-parameter consists of the magnitude and phase angle. Therefore, for this work, a data set is defined as the set of 10001 S_{21} coefficients collected across one frequency sweep. Each test run will consist of 11 data sets,

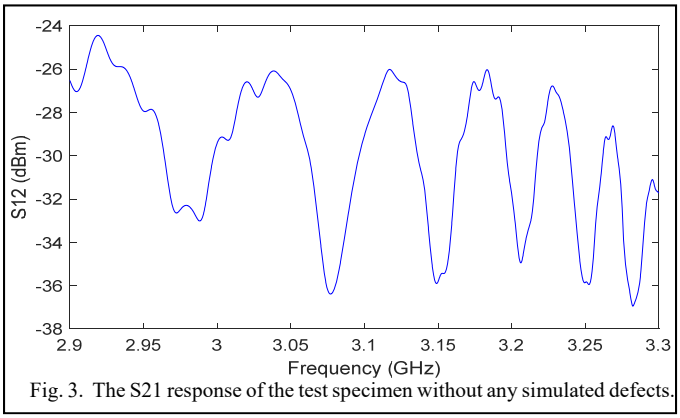

Fig. 3. The S21 response of the test specimen without any simulated defects.

where each run starts and ends with a dataset where there is no simulated defect present, and nine data sets where a simulated defect is placed within a groove at various locations. The S_{11} log magnitude response for the case without a simulated defect is given in Fig. 3.

To simulate defects, small pieces of solid aluminum wire were placed within the grooves of the test specimen. There were 15 simulated defects of five lengths: 2 mm, 5 mm, 10 mm, 15 mm and 25 mm long (Fig. 4). The wires were 1.6 mm, 2.3 mm and 3.6 mm in diameter. The aluminum wires are placed one at a time inside of the grooves roughly in the center side to side, against the back wall to simulate a filet or other extra material remaining after fabrication.

The EM response of the plasmon system across the band of interest was recorded and analyzed for multiple cases with and without simulated defects. The simulated defects are placed singly in random order at locations from 100 mm to 900 mm in 100 mm increments. For this work, it was experimentally determined that the impedance response yields the best data. The impedance was calculated from the S_{21} measurement using:

$$Z = Z_0 \frac{2(1-S_{21})}{(S_{21})} . \quad (1)$$

Where Z_0 is 50 Ω. To highlight the variance in the defect states, the change or delta impedance for our measurements is calculated using the baseline subtraction method:

$$\Delta Z = Z_i - Znd_i , \quad (2)$$

where Z_i is the current data set with or without a defect and Znd_i is the first data set without a defect. The delta impedance (ΔZ) data for nine data sets with a simulated defect (2 mm long, 1.6 mm in diameter) randomly placed at locations from 100 mm to 900 mm in 100 mm increments, are given in Fig. 5. The difficulty in discriminating differing defects led us to investigate alternate methods of post processing.

To develop a useful indication for detection of defects within grooves of the test specimen, a method of dimensionality reduction was needed. Several methods were investigated; however, a simple summation of the delta impedance across the frequency range provides acceptable results. The summation of the delta impedance across 10001 points of a data set is given by:

$$SZ = \sum_{i=1}^{10001} (\Delta Z_i) . \quad (3)$$

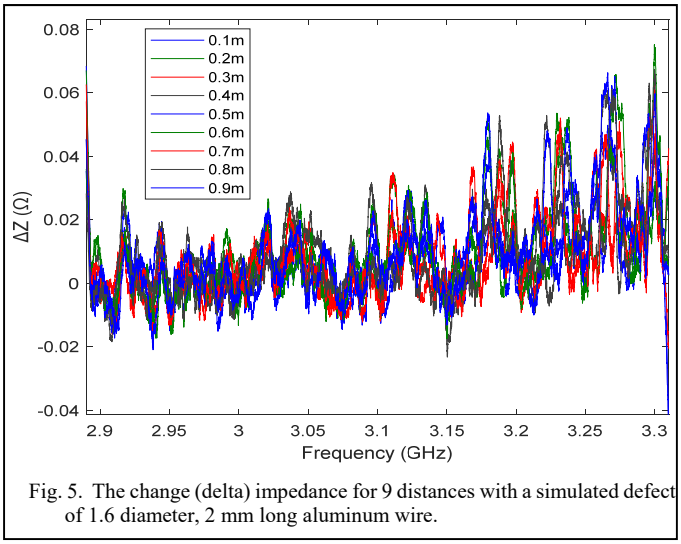

Fig. 5. The change (delta) impedance for 9 distances with a simulated defect of 1.6 diameter, 2 mm long aluminum wire.

III. Results

The sum of the delta impedance data sets, for each of the fifteen simulated defects are given in Fig. 6. For each defect case, the nine location data sets and two data sets without a defect were taken. Note that the larger the defect volume the larger the response.

The sum of the delta impedance for each defect is roughly the same for each of the nine locations. For defect detection, a threshold value of 50Ω is suggested for defects similar to those simulated. Using that number, even the smallest simulated defect of 1.6 mm diameter and 2 mm long can be detected without any false positives. In addition to detecting a defect, the sum of the delta impedance can be used to estimate the volume of the defect. The averaged sum of the delta impedance values (x) are fitted to the calculated volume using a sum of sines fit to the calculated volume. The fitted volume (V*f*(*x*)) is given by:

$$Vf(x) = a1 * sin(b1 * x + c1) + a2 * sin(b2 * x + c2) + a3 * sin(b3 * x + c3) + a4 * sin(b4 * x + c4) + a5 * sin(b5 * x + c5) + a6 * sin(b6 * x + c6) . \quad (4)$$

The averaged fitted values and the calculated volume are shown in Fig. 7.

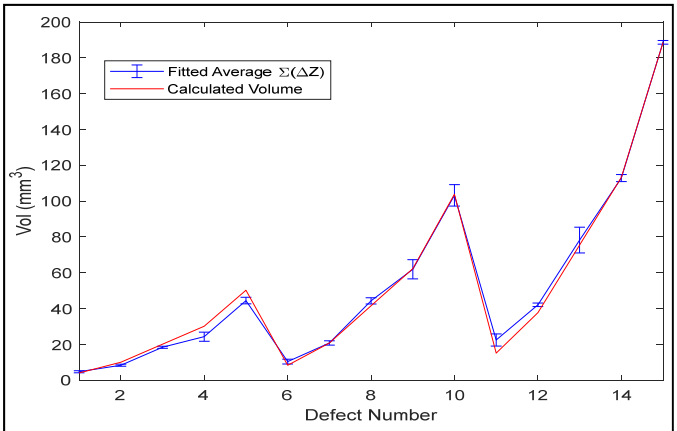

Fig. 7. The fitted average sum of delta values for all 15 defect cases. The error bars represent one standard deviation.

The fit is evaluated using the standard R-square technique. R-square is defined as the ratio of the sum of squares of the regression. In this case the R-squared value for the given parameters is 0.9920.

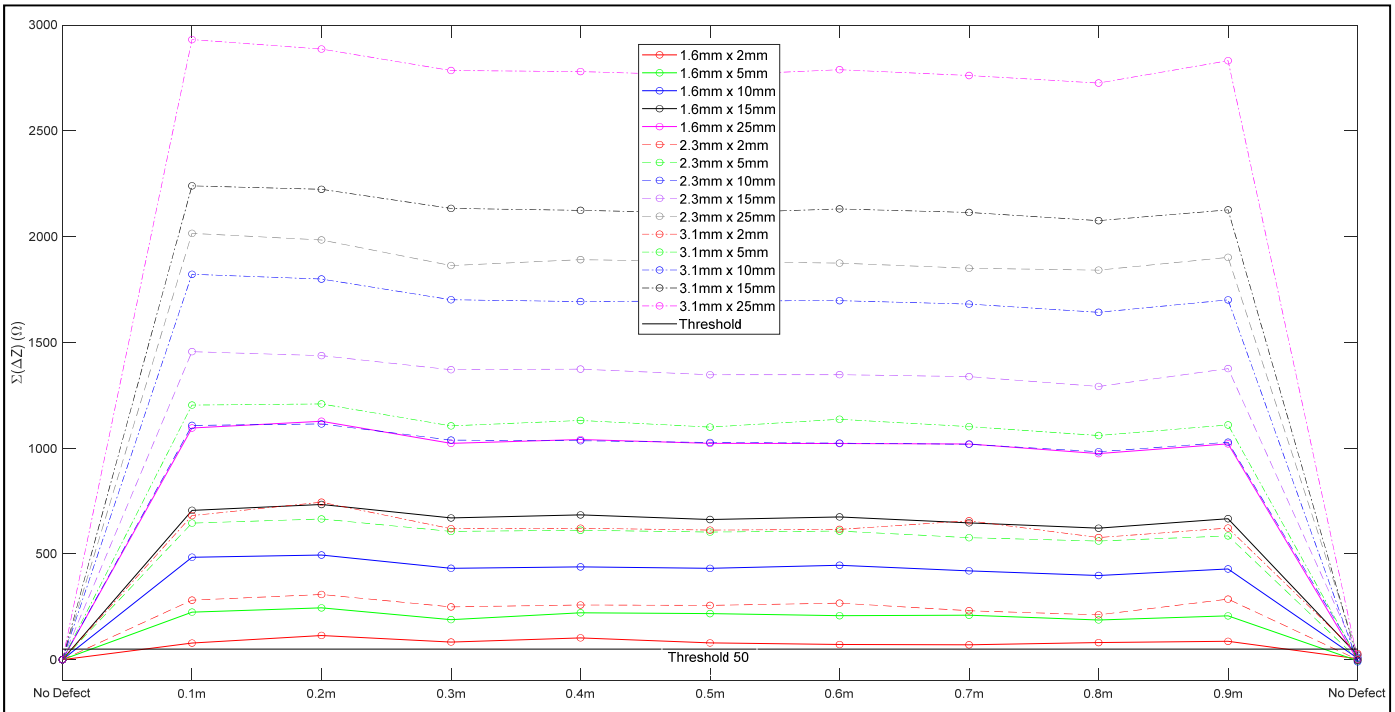

Fig. 6. The sum of the change (delta) impedance at multiple locations with a wires segments simulating defects. The black line represents the threshold for defect detection. The simulated defects are Al wires that are 1.6, 2.3 and 3.1 mm in diameter, and are 2, 5, 10, 15, and 25 mm in length.

The parameters for the fitting are given in Table I.

TABLE I. FIT PARAMETERS

Parameter	Value
a1	187.8
b1	0.6688
c10	0.4422
a2	77.72
b2	1.229
c2	-2.67
a3	3.421
b3	4.168
c3	-0.5842
a4	1.058e+04
b4	6.389
c4	2.084
a5	1.058e+04
b5	6.39
c5	-1.058
a6	5.713
b6	9.467
c6	3.241

The average fitted vales are close to the calculated volume values. The defect cases, diameter length, volume, and fitted values and the average fitted values from Eqn. (4) are given in Table II.

TABLE II. DEFECT PARAMETERS

Defect Number	Diameter (mm)	Length (mm)	Calculated Volume (mm^3)	Averaged Fit $\Sigma(\Delta Z)$ (mm^3)
1	1.6	2	4.02	4.64
2	1.6	5	10.05	9.64
3	1.6	10	20.11	19.46
4	1.6	15	30.16	30.13
5	1.6	25	50.27	50.30
6	2.3	2	8.31	8.15
7	2.3	5	20.77	21.11
8	2.3	10	41.55	42.61
9	2.3	15	62.32	62.19
10	2.3	25	103.87	103.72
11	3.1	2	15.10	15.26
12	3.1	5	37.74	37.06
13	3.1	10	75.48	76.15
14	3.1	15	113.22	112.88
15	3.1	25	188.69	188.91

CONCLUSIONS

The use of spoof plasmon polaritons for defect detection has been demonstrated using simulated defects (wires placed in a grooved metal surface). The sum of the change in the impedance technique has been utilized as the indication for detecting the different sizes of simulated inclusions. A threshold value of 50Ω has been proposed for detection of these inclusion type defects. In addition, the technique estimates the volume of the defect. Future work will investigate voids and cracks to determine if the technique will detect more defects types.

REFERENCES

[1] M. C. Stoner, A. H. Hehir, M. L. Ivanco and M. S. Domack, "Cost-Benefit Analysis for the Advanced Near Net Shape Technology (ANNST) Method for Fabricating Integrally Stiffened Cylinders," in *AIAA SPACE 2016 Forum*, Long Beach, CA, Sept. 13-16, 2016.

[2] J. B. Ransom, B. J. Jensen and E. H. Glaessgen, "ARMD Workshop on Materials and Methods for Rapid Manufacturing for Commercial and Urban Aviation," Hampton, VA, USA, Nov. 2019.

[3] W. A. Tayon, M. S. Domack and J. A. Wagner, "Characterization of 10-ft. Diameter Aluminum Alloy 2219 Integrally Stiffened Cylinders," NASA Langley Research Center, Hampton, VA, March, 2019.

[4] E. M. G. Brock, "The Lateral Confinement of Microwave Surface Waves," PhD, Dept. of Physics and Astronomy, Univ. of Exeter, pp. 1-190, 2013.

[5] H. Xiang, Y. Meng, Q. Zhang, F. F. Qin, J. J. Xiao, D. Han and W. Wen, "Spoof Surface Plasmon Polaritons on Ultrathin Metal Strips with Tapered Grooves," *Optics Communications,* vol. 356, pp. 59-63, 2017.

[6] R. S. Anwar, L. Mao and H. Nin, "Role of Surface Geometric Patterns and Parameters in the Dispersion Relations of Spoof Surface Plasmon Polaritons at Microwave Frequency," *Applied Computational Electromagnetics Society Journal,* vol. 34, no. 1, pp. 172-179, 2019.

[7] Z. Gao, X. Zhang and L. Shen, "Wedge Mode of Spoof Surface Plasmon Polaritons at Terahertz Frequencies," *Journal of Applied Physics,* vol. 108, no. 11, (113104), pp. 1-4, 2010.

[8] R. K. Jaiswal, N. Pandit and N. P. Pathak, "Spoof Surface Plasmon Polariton-Based Reconfigurable Band-Pass Filter using Planar Ring Resonator," *Plasmonics,* vol. 14, no. 3, pp. 631-646, 2019.

[9] Y. G. Ma, L. Lan, S. M. Zhong and C. K. Ong, "Experimental Demonstration of Subwavelength Domino Plasmon Devices for Compact High-Frequency Circuit," *Optics Express,* vol. 19, no. 22, pp. 21189-21198, 2011.

[10] B. Ng, S. M. Hanham, J. Wu and et al., "Broadband Terahertz Sensing on Spoof Plasmon Surfaces," *ACS Photonics,* vol. 1, no. 10, pp. 1059-106, 2014.

[11] Z. Gao, F. Gao, H. Xu, Y. Zhang and B. Zhang, "Localized Spoof Surface Plasmons in Textured Open Metal Surfaces," *Optics Letters,* vol. 41, no. 10, pp. 2181-2184, 2016.

[12] F. J. Zucker, "Theory and Applications of Surface Waves," *Il Nuovo Cimento,* vol. 9, no. 3, pp. 450-473, 1952.

[13] A. K. Klein, A. Basden, J. Hamml and et al., "Scattering of Spoof Surface Plasmon Polaritons in Defect-Rich THz Waveguides," *Scientific Reports,* vol. 9, no. 1, pp. 1-8, 2019.

[14] Z. Xie, L. Sun, F. Wu and et al, "Applying Spoof Surface Plasmons to Non-Destructive Testing," in *IEEE 3rd Advanced Information Technology, Electronic and Automation Control Conference (IAEAC)*, Chongqing, China, pp. 330-333, Oct. 12-14, 2018.

[15] X. Yang, J. Chen, P. Su and et al, "Detection of Defects in Film-Coated Metals and Non-Metallic Materials Based on Spoof Surface Plasmon Polaritons," *IEEE Sensors Journal,* vol. 19, no. 24, pp. 11891-11899, 2019.

[16] P. Su, X. Yang, J. Wang and et al, "Su, Piqiang, Xiaoqing Yang, Jun Wang, Zhendong Wang, Huajiang Peng, and Jianping Yuan. "Method of Defects Detection in Non-metallic Composites Based on Liquid Flow Controlled Spoof Surface Plasmon Polaritons," *IEEE Sensors Journal,* vol. 21, no. 12, pp. 13239-13246, 2021.